ıd that they now with proper
performance.
ɔl that is a driving factor. A
) which is an old idea, but it
ıns or analog electronics. Now
ıad.

: above will be in focus. The
osis functionality are steadily
areas that help meeting the
ɔl and diagnosis functions in
have to be obtained not only
of time. Other examples are
improved driveability due to
e.g. reduce clutch wear.
ıtical models will play an im-
ıtrol and diagnosis. They will
ntrol, and supervision.

ehicle designs. It will also to
ı design leading to:

ıre made possible by, and rely

: mechanics and control. The
e perspectives on automotive
ıpiring mind teaser:

air cleaner for usual town air.
typically somewhat polluted
house heating and industries.
t emissions are such that the
n be lower than in town air.
have been combusted or have

vater and carbon dioxide, the
uel consumption.
heavily on automotive con-
ıir cleaner under all possible
This is a mind teaser, but
ep.

2 Thermodynamic Engine Cycles

In this chapter, the thermodynamic characteristics of basic engine cycles are explained. For each concept, the thermal efficiency is derived from thermodynamic equations. An introduction into Thermodynamics can be found in Appendix A.1.

2.1 Ideal Combustion Engines

Commonly used combustion engines in cars are four-stroke engines. They have two intermittent cycles: the gas is compressed, combusted and expanded in the first cycle, and the gas is exchanged in the second cycle. In this section the second (or passive) cycle will not be considered to simplify the mathematical derivations. The processes related to the second cycle will be discussed in Chapter 3.

Two different types of combustion engines have to be distinguished:

1. Spark-ignited Engine: Combustion caused by an electric spark-ignition.
2. Diesel Engine: Combustion caused by self inflammation due to compressional heat.

In most sections, p represents the in-cylinder pressure, V the cylinder volume, ϑ the in-cylinder temperature, S the entropy, q the thermal energy of the gas, u it's internal energy and h it's enthalpy.

2.1.1 Spark-ignited (SI) Engine

The first SI engine was presented by Nikolaus Otto in 1862. The combustion process can be modelled as an **isochoric process** where the gas volume is considered to be constant. The pV-diagram in Figure 2.1 illustrates that the gas

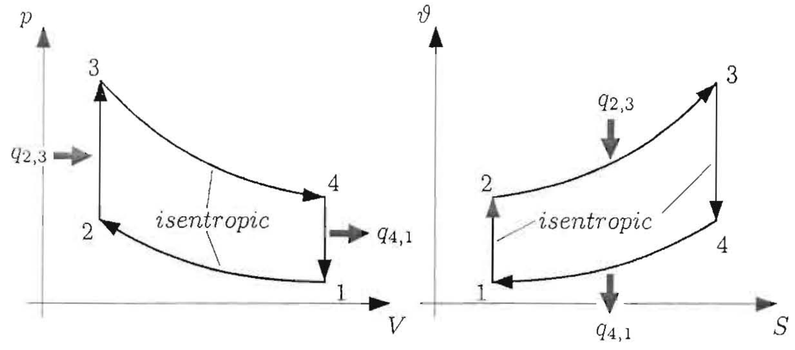

Figure 2.1 pV-diagram (left) and ϑS-diagram (right) of the SI engine process

volume does not change between step 2 and step 3. The ratio of maximum to minimum volume is given by:

$$\varepsilon = \frac{V_1}{V_2} \tag{2.1}$$

This ratio ε is called the **compression ratio** of the engine. The different steps for a complete cycle in the pV-diagram and in the ϑS-diagram can be seen in Figure 2.1. Mathematically they can be described as followed:

$1 \to 2$: Isentropic compression, $dq = 0$:

$$\begin{aligned} dq &= du + dw = 0 \\ q_{1,2} &= 0 \\ dw &= -du = -m\,c_v\,d\vartheta \\ w_{1,2} &= -\int_1^2 m\,c_v\,d\vartheta = -m\,c_v(\vartheta_2 - \vartheta_1) \end{aligned}$$

The work $w_{1,2}$ is used to compress the gas and therefore, it is negative.

$2 \to 3$: Isochoric input of thermal energy, $dV = 0$:

$$\begin{aligned} dw &= p\,dV = 0 \\ w_{2,3} &= \int_2^3 p\,dV = 0 \\ dq &= du = m\,c_v\,d\vartheta \\ q_{2,3} &= m\,c_v \int_2^3 d\vartheta = m\,c_v(\vartheta_3 - \vartheta_2) \end{aligned}$$

The increased thermal energy $q_{2,3}$ is caused by combustion of the gas.

$3 \to 4$: Isentropic ex

This state chan
the output of ki

$4 \to 1$: Isochoric hea

The loss of the
gas is pumped
a cold mixture
$\vartheta_1 < \vartheta_4$).

The thermal efficienc
energies to the inpu
cycle:

The relationship for
the equation:

This yields:

$3 \rightarrow 4$: Isentropic expansion, $dq = 0$:

$$
\begin{aligned}
q_{3,4} &= 0 \\
dw &= -du = -m\,c_v\,d\vartheta \\
w_{3,4} &= -\int_3^4 m\,c_v\,d\vartheta = -m\,c_v(\vartheta_4 - \vartheta_3)
\end{aligned}
$$

This state change describes the power stroke of the engine where $w_{3,4}$ is the output of kinetic energy from the gas, which is positive ($\vartheta_4 < \vartheta_3$).

$4 \rightarrow 1$: Isochoric heat loss, $dV = 0$:

$$
\begin{aligned}
dw &= p\,dV = 0 \\
w_{4,1} &= \int_4^1 p\,dV = 0 \\
dq &= du + dw = m\,c_v\,d\vartheta \\
q_{4,1} &= m\,c_v \int_4^1 d\vartheta = m\,c_v(\vartheta_1 - \vartheta_4)
\end{aligned}
$$

The loss of thermal energy $q_{4,1}$ is due to the gas exchange: The burnt hot gas is pumped into the exhaust and the combustion chamber is filled with a cold mixture of unburnt fuel vapour and air ($q_{4,1}$ is negative because of $\vartheta_1 < \vartheta_4$).

The thermal efficiency of the engine is equivalent to the ratio of all the kinetic energies to the input of thermal energy $q_{2,3}$ at the combustion of a complete cycle:

$$
\begin{aligned}
\eta_{th} &= \frac{w_{1,2} + w_{2,3} + w_{3,4} + w_{4,1}}{q_{2,3}} \\
&= \frac{m\,c_v(-\vartheta_2 + \vartheta_1 - \vartheta_4 + \vartheta_3)}{m\,c_v(\vartheta_3 - \vartheta_2)} \\
&= 1 - \frac{\vartheta_4 - \vartheta_1}{\vartheta_3 - \vartheta_2} \\
&= 1 - \frac{\vartheta_1}{\vartheta_2}\,\frac{\vartheta_4/\vartheta_1 - 1}{\vartheta_3/\vartheta_2 - 1}
\end{aligned}
$$

The relationship for isentropic changes $1 \rightarrow 2$ and $3 \rightarrow 4$ can be used to simplify the equation:

$$
\frac{\vartheta_4}{\vartheta_3} = \left(\frac{V_3}{V_4}\right)^{\kappa-1} = \frac{1}{\varepsilon^{\kappa-1}} = \frac{\vartheta_1}{\vartheta_2} \tag{2.2}
$$

This yields:

$$
\eta_{th} = 1 - \frac{1}{\varepsilon^{\kappa-1}} \tag{2.3}
$$

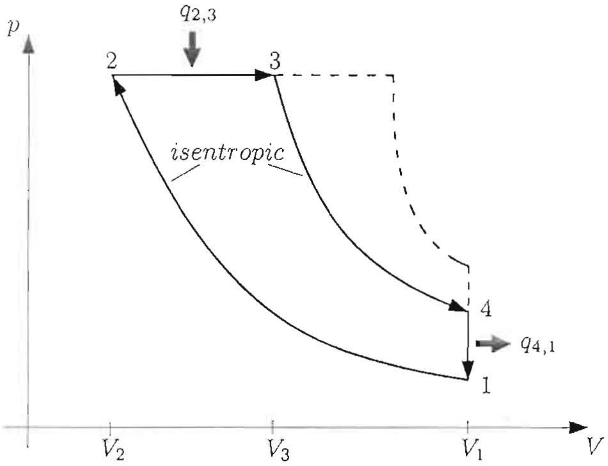

Figure 2.2 pV-diagram for Diesel Engine

Please note that the thermal efficiency η_{th} does not depend on the absolute temperature values. It mainly depends on the compression ratio ε. Example: For a compression ratio of $\varepsilon = 11$ and an adiabatic coefficient of $\kappa = 1.4$ the theoretical thermal efficiency η_{th} is:

$$\eta_{th} = 0.617$$

2.1.2 Diesel Engine

Rudolf Diesel developped this engine from 1893 to 1897. In a diesel engine, the combustion takes place in an **isobaric state change** during the downward movement of the piston. At the beginning of this process the combustion is controlled by the injection of fuel to maintain a constant pressure at the expansion from 2 to 3. The isobaric state change is indicated between steps 2 and 3 in the pV-diagram in Figure 2.2. The more fuel is injected, the longer the distance between steps 2 and 3 and the larger the volume ratio:

$$\rho = \frac{V_3}{V_2} = \frac{\vartheta_3}{\vartheta_2} \quad . \tag{2.4}$$

This ratio is called **injection ratio** or **load**. The injection ratio ρ has an impact on the thermodynamic efficiency which is derived after explaining the different parts of the cycle:

$1 \rightarrow 2$: Isentropic compression, $dq = 0$:

$$\begin{aligned} dq &= du + dw = 0 \\ q_{1,2} &= 0 \\ dw &= -du = -m\,c_v\,d\vartheta \\ w_{1,2} &= -m\,c_v(\vartheta_2 - \vartheta_1) \end{aligned}$$

The mechanical work u
engine). It is negative.

$2 \rightarrow 3$: Isobaric gain of ther

In this process, the con
duces the kinetic energ

$3 \rightarrow 4$: Isentropic expansion

Note that $w_{3,4}$ is posit

$4 \rightarrow 1$: Isochoric heat loss,

Note that $q_{4,1}$ is negat

With $\kappa = \frac{c_p}{c_v}$ and $R = (c_p - c$
can now be calculated:

This equation can be simplifi
(Eq. 2.2) and the relationsh
the following relationship is

production
:ng operation

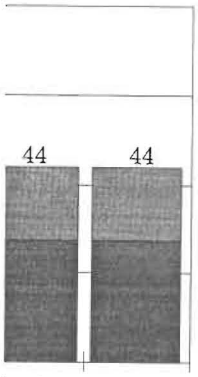

'uel cell engine
with with
ıdrogen methanol

ine concepts [45]

ications at short distances. :re an internal combustion ectrical motor may be ac- engine and the driveline, t load conditions the com- ery volume and weight are

adequate energy source. It re of 20 K or at relatively periods, H_2 leaks through s chemically bound. Since nissions of nitrogen oxyde

w temperatures. Thermal $_2$ and O_2. The storage of er generated from natural :. The task is to generate n under realtime transient can be modelled, and the stimated in realtime, as a a promising alternative to y requirements to move a ystems.

3 Engine Management Systems

3.1 Basic Engine Operation

3.1.1 Effective Work

Four-stroke engines are characterised by two alternate cycles: In the first cycle, equivalent to the first and second strokes, the gas is compressed, combusted and expanded. In the second cycle, equivalent to the third and fourth strokes, the gas is transferred to the exhaust pipe and the cylinder is filled with fresh air from the intake manifold. Figure 3.1 shows the two cycles. The crankshaft is turned 360° per cycle. SI and diesel engines are controlled differently: In diesel engines, fuel is directly injected into the combustion chamber. The amount of injected fuel per stroke is then proportional to engine torque. The amount of air is almost constant at a given speed. In SI engines, the amount of fuel as well as air is controlled. When the fuel is injected into the intake manifold, a homogeneous air-fuel mixture is sucked into the cylinders. The mechanical work generated in the combustion cycle can be obtained by an integration in the pV-diagram. The mechanical work can be normalised by dividing by the displacement volume V_d:

$$w_i = \frac{1}{V_d} \sum_{j=1}^{CYL} \oint \Big(p_j(V_j) - p_0\Big) dV_j \quad , \tag{3.1}$$

where:

$V_d = CYL \cdot (V_1 - V_2)$	is the displacement volume of all cylinders
CYL	is the number of cylinders
w_i	is the (normalised) indicated specific work.

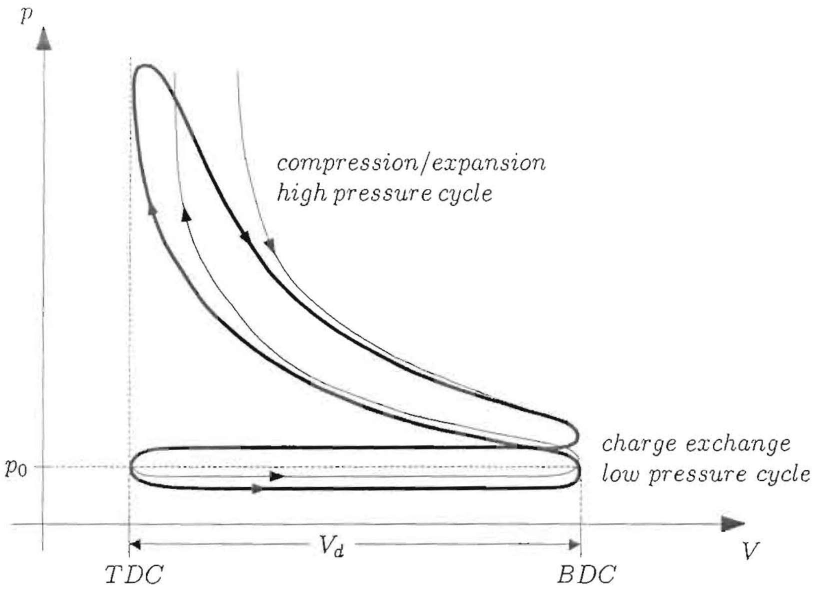

Figure 3.1 pV-diagram of four-stroke combustion engine

The value of w_i can be determined by measuring the in-cylinder pressure during a cycle. An indicated specific work of $1\,J/cm^3$ is equivalent to a mean pressure of $\bar{p} = 10\,bar$ $(= 10^6\,Pa)$. Dealing with a four-stroke engine, the measurement has to last for two cycles. The transfer of the combustion torque to the engine torque available at the crankshaft can be calculated from the following motion equations.

The piston stroke from Top Dead Center (TDC) is

$$s(\alpha_{CS}) = l(1 - \cos\beta) + r(1 - cos\alpha_{CS}) \quad .$$

From Figure 3.2 we get

$$\begin{aligned} l \sin\beta &= r \sin\alpha_{CS} \quad , \\ \cos\beta &= \sqrt{1 - \frac{r^2}{l^2}\sin^2\alpha_{CS}} \quad , \end{aligned} \tag{3.2}$$

which yields the piston stroke as

$$s(\alpha_{CS}) = r\left(1 - cos\alpha_{CS} + \frac{l}{r}\left(1 - \sqrt{1 - \frac{r^2}{l^2}\sin^2\alpha_{CS}}\right)\right) \quad . \tag{3.3}$$

At Top Dead Center, we have $\alpha_{CS} = 0$, $s(\alpha_{CS}) = 0$, and at Bottom Dead Center on

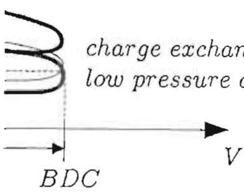

ıbustion engine

in-cylinder pressure during
ıalent to a mean pressure of
.gine, the measurement has
torque to the engine torque
following motion equations.

$\alpha_{CS})$.

, (3.2)

$\sin^2 \alpha_{CS} \Big)\Big)$. (3.3)

nd at Bottom Dead Center

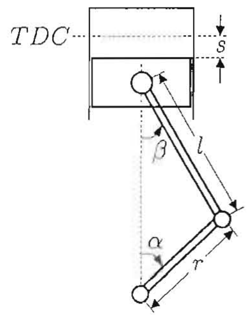

s : *piston stroke*
r : *crankshaft radius*
α_{CS} : *crankshaft angle*
l : *connecting rod length*

Figure 3.2 Piston and crankshaft motion

$\alpha_{CS} = \pi$, $s(\alpha_{CS}) = 2r$ respectively. The derivatives of the piston stroke are

$$\frac{ds}{d\alpha_{CS}} = r\left(\sin\alpha_{CS} + \frac{r}{l}\cdot\frac{\sin\alpha_{CS}\cos\alpha_{CS}}{\sqrt{1-\frac{r^2}{l^2}\sin^2\alpha_{CS}}}\right)$$

and

$$\frac{d^2s}{d\alpha_{CS}^2} = r\left(\cos\alpha_{CS} + \frac{\frac{r}{l}(\cos^2\alpha_{CS} - \sin^2\alpha_{CS}) + \frac{r^2}{l^2}\sin^4\alpha_{CS}}{\left(\sqrt{1-\frac{r^2}{l^2}\sin^2\alpha_{CS}}\right)^3}\right) \quad . \tag{3.4}$$

These derivatives over crankshaft angle can be related to the derivatives over time as follows:

$$\begin{aligned}
\dot{s} &= \frac{ds}{dt} = \frac{ds}{d\alpha_{CS}}\cdot\frac{d\alpha_{CS}}{dt} = \frac{ds}{d\alpha_{CS}}\cdot\dot{\alpha}_{CS} \\
\ddot{s} &= \frac{d^2s}{dt^2} = \frac{d}{dt}\left(\frac{ds}{d\alpha_{CS}}\cdot\frac{d\alpha_{CS}}{dt}\right) = \frac{d}{dt}\left(\frac{ds}{d\alpha_{CS}}\right)\cdot\frac{d\alpha_{CS}}{dt} + \frac{ds}{d\alpha_{CS}}\cdot\frac{d^2\alpha_{CS}}{dt^2} \\
&= \frac{d^2s}{d\alpha_{CS}^2}\cdot\dot{\alpha}_{CS}^2 + \frac{ds}{d\alpha_{CS}}\cdot\ddot{\alpha}_{CS}
\end{aligned} \tag{3.5}$$

The indicated specific work can be written as

$$\begin{aligned}
w_i &= \frac{1}{V_d}\oint\sum_{j=1}^{CYL}(p_j(\alpha_{CS}) - p_0)\,A_p\,\frac{ds_j(\alpha_{CS})}{d\alpha_{CS}}d\alpha_{CS} \\
&= \frac{1}{V_d}\oint T_{comb}(\alpha_{CS})d\alpha_{CS} \quad .
\end{aligned} \tag{3.6}$$

The combustion torque at the crankshaft is thus defined as

$$T_{comb}(\alpha_{CS}) = \sum_{j=1}^{CYL}(p_j(\alpha_{CS}) - p_0)\,A_p\,\frac{ds_j}{d\alpha_{CS}} \quad . \tag{3.7}$$

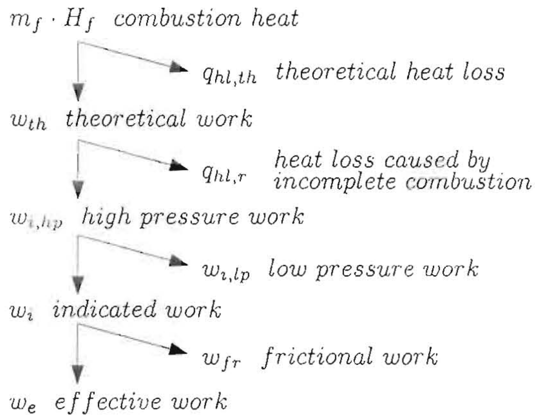

Figure 3.3 The effective work delivered by the engine is much lower than the thermal energy caused by combustion.

The piston strokes in different cylinders are shifted by phase.

$$s_j(\alpha_{CS}) = s\left(\alpha_{CS} - (j-1)\cdot\frac{4\pi}{CYL}\right) \quad , \quad j = 1, ..., CYL \tag{3.8}$$

The average combustion torque is

$$\begin{aligned} \bar{T}_{comb} &= \frac{1}{4\pi}\oint T_{comb}(\alpha_{CS})d\alpha_{CS} \\ &= \frac{P_i}{\dot{\alpha}_{CS}} \quad , \end{aligned} \tag{3.9}$$

where P_i is the mean indicated power. The total indicated work $w_i V_d$ can now be written at stationary engine operation as

$$w_i V_d = 4\pi\bar{T}_{comb} = 4\pi\frac{P_i}{\dot{\alpha}_{CS}} = \frac{4\pi P_i}{2\pi n} = \frac{2P_i}{n} \quad ,$$

and the normalised work

$$w_i = \frac{2P_i}{V_d\, n} \quad , \tag{3.10}$$

where $n = \dot{\alpha}_{CS}/(2\pi)$ is the engine speed. In reality, the effective work w_e per volume is much lower than the indicated work w_i (see Figure 3.3). The effective thermodynamic efficiency η_e is at constant fuel flow

$$\eta_e = \frac{P_e}{\dot{m}_f\, H_f} = \frac{w_e\, V_d\, n}{2 m_f\, n\, H_f}\cdot\frac{2}{CYL} = \frac{w_e}{m_f\, H_f}\cdot\frac{V_d}{CYL} \quad . \tag{3.11}$$

where:

P_e	is the effective p
w_e	is the effective s
m_f	is the mass of fu
$\dot{m}_f$	is the fuel flow i
H_f	is the specific en
V_d	is the total displ
	(V_d/CYL displa

The indicated thermodyna

Some examples of typical v

Table 3.1 Indicated specifi loss $q_{hl,r}$ for different engine

Engine Ty
w_i
$q_{hl,th}$
$q_{hl,r}$

3.1.2 Air-Fuel Rat

The ratio of air to fuel is nal combustion engines. amount of air m_a transfer throttle butterfly, aerodyn rebounding of already bur other effects. The amount volume V_d under the norm density $\rho_0 = 1.29\,kg/m^3$ theoretical value is equival

Similarly, the ratio of mea equivalent to the relative f

P_e	is the effective power in W
w_e	is the effective specific work per cycle in J/m^3
m_f	is the mass of fuel measured per cylinder in kg
$\dot{m}_f$	is the fuel flow in kg/s
H_f	is the specific energy of the fuel released in the combustion J/kg
V_d	is the total displacement volume in m^3 (V_d/CYL displacement volume per cylinder)

The indicated thermodynamic efficiency (friction not considered) is:

$$\eta_i = \frac{w_i}{2m_f H_f} \cdot \frac{V_d}{CYL} \tag{3.12}$$

Some examples of typical values for the indicated efficiency are given in table 3.1.

Table 3.1 Indicated specific work w_i, theoretical heat loss $q_{hl,th}$, and realistic heat loss $q_{hl,r}$ for different engine types, related to fuel combustion heat.

Engine Type	SI	Diesel	Big Diesel
w_i	33-35 %	40-43 %	45-48 %
$q_{hl,th}$	23-28 %	22-25 %	12-14 %
$q_{hl,r}$	37-44 %	35-40 %	26-33 %

3.1.2 Air-Fuel Ratio

The ratio of air to fuel is very important for the combustion process of internal combustion engines. There are several effects that have an impact on the amount of air m_a transferred to the cylinder: Throttling of the air flow by the throttle butterfly, aerodynamic resistance and resonances in the intake manifold, rebounding of already burned gases from the cylinder into the inlet pipes and other effects. The amount of air which would theoretically fit into a displacement volume V_d under the normalised pressure $p_0 = 1.013\,bar$ and the normalised air density $\rho_0 = 1.29\,kg/m^3$ is expressed by $m_{a,th} = \rho_0 V_d$. The ratio of real to theoretical value is equivalent to the relative air supply:

$$\lambda_a = \frac{m_a}{m_{a,th}} \tag{3.13}$$

Similarly, the ratio of measured fuel mass m_f to theoretical fuel mass $m_{f,th}$ is equivalent to the relative fuel supply:

$$\lambda_f = \frac{m_f}{m_{f,th}} \tag{3.14}$$

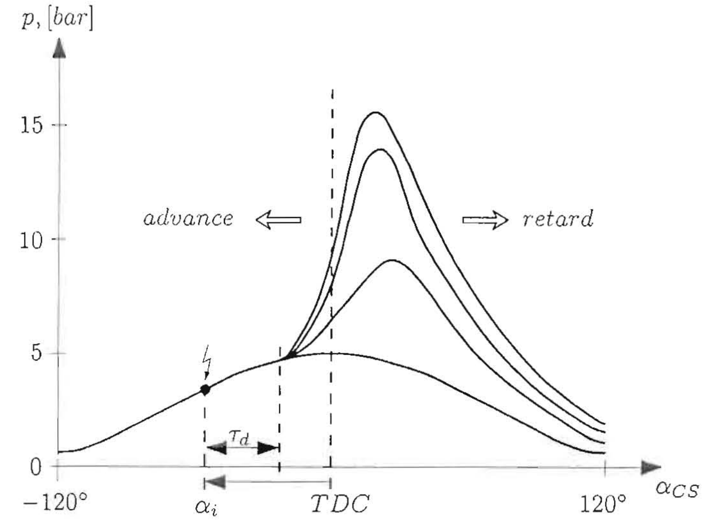

Figure 3.9 In-cylinder pressure p over crankshaft angle α_{CS}.

The gas is compressed by the piston in an approximately isentropic process. With ignition at α_i, the pressure rises only after time lag τ_d. The maximum pressure varies from cycle to cycle. The inflammation lag τ_d depends on temperature, pressure, air-fuel ratio and self inflammation time as described in the previous section. It also depends on the type of fuel being used. Figure 3.10 shows some inflammation lags for different fuels over temperature. Oil companies adapt their fuel to weather conditions (summer, winter).

Turbulence caused by the upward moving piston has no impact on the time lag τ_d. For a correct ignition angle, this lag must be considered. The time lag is convoluted to an angle lag, increasing proportional to engine speed. Contrary to that, the engine speed has almost no impact on the position of energy conversion as turbulences increase the transport velocity with higher engine speeds.

The energy conversion caused by combustion is shown in Figure 3.11 for different air-fuel ratios λ. In these curves, the isentropic pressure curves are suppressed. The differential output of thermal energy per angle $dE/d\alpha_{CS}$ (its gradient) is normalised to the total thermal energy E_0. The shape of the relative energy conversion is therefore almost constant.

If the air-fuel ratio is increased e.g. to $\lambda = 1.2$ as shown in Figure 3.11, the ignition lag τ_d will rise. At a constant ignition angle α_{i1} the energy conversion is then retarded. Therefore, the ignition angle must be advanced to α_{i2}, to compensate for the increased delay. The energy conversion returns to its previous position. It should be mentioned that a high air-fuel ratio λ increases the variance of the time lag τ_d.

The ignition angle α_i depends on λ which can be seen in Figure 3.12. The angle is computed by averaging the energy conversion over 0.1 %, 1 %, 10 %, 50 %,

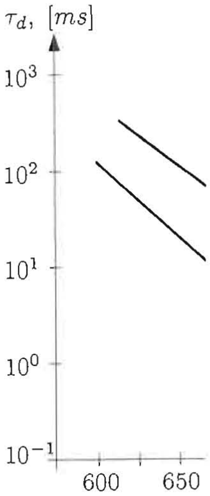

Figure 3.10 Inflammat

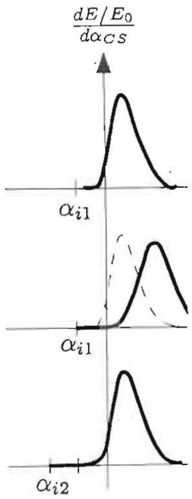

Figure 3.11 Normalised energ
ratios λ.

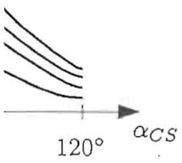

ıaft angle α_{CS}.

ıately isentropic process.
; τ_d. The maximum pres-
depends on temperature,
lescribed in the previous
Figure 3.10 shows some
)il companies adapt their

.s no impact on the time
ısidered. The time lag is
ıgine speed. Contrary to
tion of energy conversion
.er engine speeds.
ıown in Figure 3.11 for
opic pressure curves are
per angle $dE/d\alpha_{CS}$ (its
The shape of the relative

hown in Figure 3.11, the
$_{i1}$ the energy conversion
be advanced to α_{i2}, to
on returns to its previous
> λ increases the variance

een in Figure 3.12. The
er 0.1 %, 1 %, 10 %, 50 %,

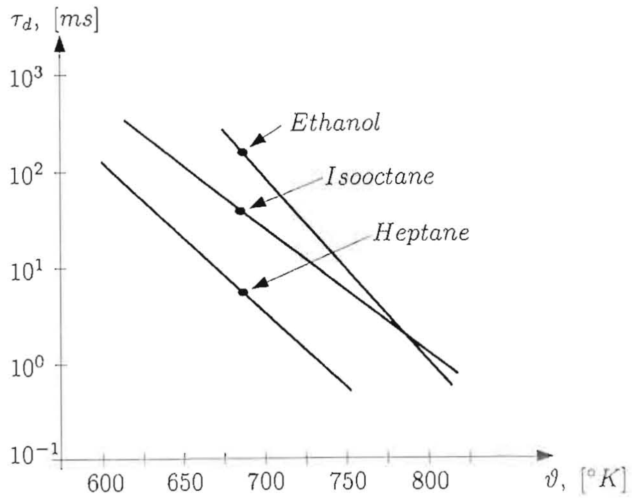

Figure 3.10 Inflammation lag τ_d over temperature for different fuels.

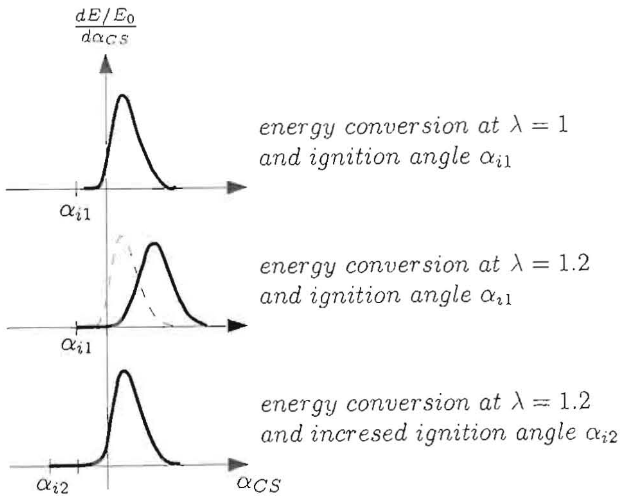

Figure 3.11 Normalised energy conversion caused by combustion for different air-fuel ratios λ.

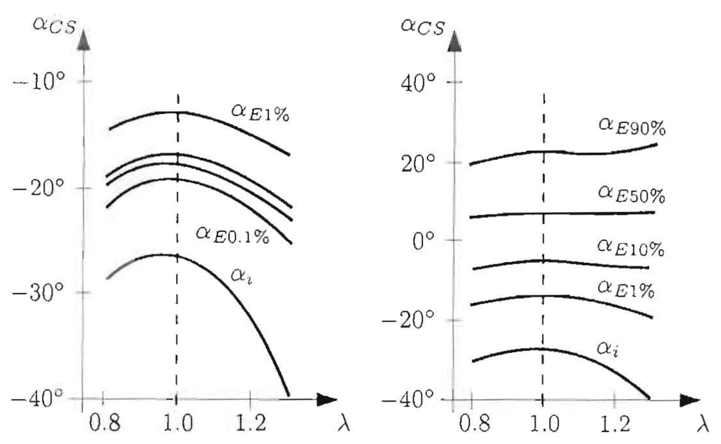

Figure 3.12 Angle α_{CS} of energy conversion over air-fuel ratio λ during ignition (left) and combustion (right) process.

90 % points. The angles for $\alpha_{E1\%}$ and higher are almost independent of the air-fuel ratio λ. In-cylinder pressure measurements can be used to control the ignition angle in a closed loop to maintain a constant position of energy conversion as shown in Figure 3.13. The angle of maximum pressure gradient $max(dp/d\alpha_{CS})$ may be used as a control variable. The controller time constant must be relatively large because of the high delay time variances between consecutive cycles. Thus closed loop ignition control may be too slow for the dynamic response of the engine.

The ignition angle is determined to find a compromise between fuel consumption, emissions or knocking. An equivalent procedure can be found for the fuel injection angle at Diesel engines.

3.2 Fuel Control

3.2.1 Emissions of Internal Combustion Engines

Mixture formation can be achieved by manifold or by in-cylinder injection. With sufficient time the mixture is distributed homogeneously in the cylinder with an air-fuel ratio in the range of $0.9 < \lambda < 1.3$. For very lean mixtures $\lambda > 1.3$, a rich stratified charge must be concentrated in a portion of the combustion chamber.

The combustion process is started by an electric spark at SI engines and by self-inflammation at Diesel engines. The inflammation is delayed as described in the previous section.

- Homogeneous mixture, stochiometric air-fuel ratio: The flame has a characteristic blue color. Almost no soot (carbon particulates) is produced.
- Stratified charge, lean air-fuel ratio: The flame has a characteristic yellow color. Soot is produced.

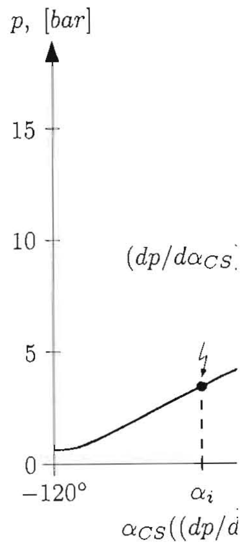

Figure 3.13 Closed-loop cont
of energy conversion.

- Inflammation starts cor

The inflammation process de
and activation energy E of t
according to the concentratio

This ratio is temperature dep
The pollutant emissions l
ratio which is shown in Figur

$\lambda < 1$: Increased emission of

$\lambda = 1$: Stochiometric combus
converter.

$\lambda \approx 1.1$: Highest nitrogen oxi
temperatures.

$\lambda > 1.1$: Decreasing nitrogen
temperatures. Increasir

$\lambda > 1.5$: Lean operation. For
verter is required.

The concentration of oxygen
air-fuel ratio λ for $\lambda \geq 1$ usin

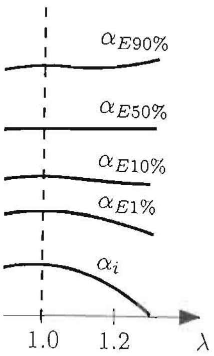

el ratio λ during ignition (left)

nost independent of the air-
e used to control the ignition
ion of energy conversion as
ure gradient $max(dp/d\alpha_{CS})$
constant must be relatively
en consecutive cycles. Thus
e dynamic response of the

mise between fuel consump-
e can be found for the fuel

n Engines

in-cylinder injection. With
usly in the cylinder with an
ean mixtures $\lambda > 1.3$, a rich
f the combustion chamber.
spark at SI engines and by
n is delayed as described in

tio: The flame has a char-
articulates) is produced.

has a characteristic yellow

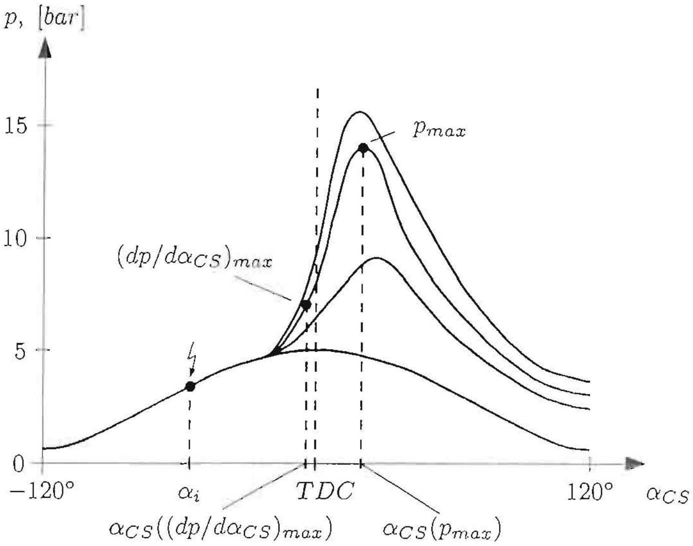

Figure 3.13 Closed-loop control of ignition angle α_i to maintain a constant position of energy conversion.

- Inflammation starts combustion from one location.

The inflammation process depends on pressure p, temperature ϑ, air-fuel ratio λ and activation energy E of the fuel. For $\lambda < 1$ the exhaust gases are generated according to the concentration ratio

$$k = \frac{n_{CO} \cdot n_{H_2O}}{n_{CO_2} \cdot n_{H_2}} \quad . \tag{3.20}$$

This ratio is temperature dependant. A typical value for $\vartheta = 1850\,°K$ is $k = 3.6$.

The pollutant emissions like CO, HC, NO_x depend strongly on the air-fuel ratio which is shown in Figure 3.14

$\lambda < 1$: Increased emission of hydrocarbon HC and carbon monoxide CO.

$\lambda = 1$: Stochiometric combustion. Very low emissions after three way catalytic converter.

$\lambda \approx 1.1$: Highest nitrogen oxide NO_x emissions due to highest combustion peak temperatures.

$\lambda > 1.1$: Decreasing nitrogen oxide NO_x concentration and lower combustion temperatures. Increasing hydrocarbon HC emissions at eventual misfires.

$\lambda > 1.5$: Lean operation. For very low emissions, a NO_x reducing catalytic converter is required.

The concentration of oxygen O_2 in the exhaust gas can be used to determine the air-fuel ratio λ for $\lambda \geq 1$ using a lambda-sensor.

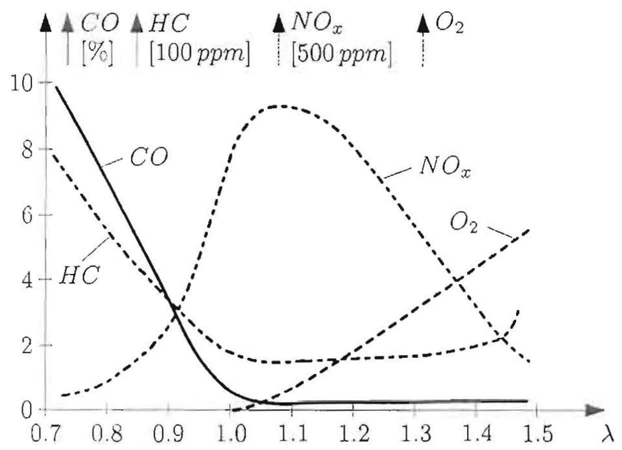

Figure 3.14 Raw emissions of CO, HC, NO_x and O_2 over air-fuel ratio λ for SI engines.

3.2.2 Fuel Measurement

The air-fuel ratio λ is an important variable for fuel control which is based on different control concepts:

rich mixture $\lambda < 1$: Maximum power per displacement volume because of increased relative fuel supply λ_f. It was used at high engine loads until 1970. Nowadays it is only used for cold engines during the warm-up phase. High emission rates.

stochiometric mixture $\lambda = 1$: Acceptable power output. This ratio is required for proper operation of three-way catalytic converters. At high engine loads, a good compromise between power output and exhaust emissions is achieved.

moderately lean mixture $1 < \lambda < 1.5$: Good efficiency because of increased air supply λ_a, but high emissions of NO_x. This method was used at part loads until 1980.

lean mixture $\lambda > 1.5$: High efficiency because of high λ_a. NO_x emissions are still high, so that catalytic converters for NO_x reduction are required. This method is used in lean-burn engines at part loads and in Diesel engines. Maximum engine power cannot be reached.

The reference torque desired by the driver controls either the relative air supply λ_a via the throttle angle α_t at SI engines or the relative fuel supply λ_f at Diesel engines. The amount of fuel being mixed with the air is regulated by the fuel control system to obtain a predefined air-fuel ratio λ. There are two different injection systems:

1. **Manifold injection:** T
front of the inlet ports.
Problems may occur at i
a low air flow velocity ir
air flow into the different
is less accurate at idling
controlled: Errors due t
on the amount of fuel i
of manifold injection is
in the cylinder at λ =
restrictions for the desig
optimised without majo
the inlet valves. The inle
at low engine speed. T
effective work w_e witho
the evaporating fuel. T
allows higher compressic
is phase-shifted for each
before the inlet valve is
can be controlled indivi
for each cylinder: limita
at coasting or cylinder s

2. **In-cylinder injection**:
The aim is to assemble
a limited portion of th
the spark plug at the ti
pressure (thus fuel atom
of injection) and the inj
point. The swirl is cont
The aim is to burn very l
injection. By an early
ing throughout the cor
to the swirl. The follo
which is burning fast w
reduced amount of the
also reduced. The earl
afterwards. Since the m
ing maximum allowable
charge, soot was genera
this can be effectively r

The total amount of injected

- aspirated air flow per ti
- intake manifold pressur
- throttle angle α_t and it

the inlet pipe and fuel flow

(3.64)

a proportional part $(1-c)$
tant T. For wall wetting
. the allocated fuel mass:

(3.65)

: $\frac{1}{1-c}$ and a time constant
the operation point of the
amic transients by varying
imized. Fig 3.20 shows test
d effectively leading to less

ent of possible disruptions
However, the consequences
wetting model is completed
time constant.

ies

ies do not require a spark
ation due to compressional
ces the ignition angle.

iting range is very impor-
s well as on emission rates.
wo phases:

se considerably within this
pends on the temperature,
ivoluted into an equivalent
eed.

l phase is almost constant
l by the piston movement,
as the combustion process.

ion angles, the emission of
tudes at advanced ignition

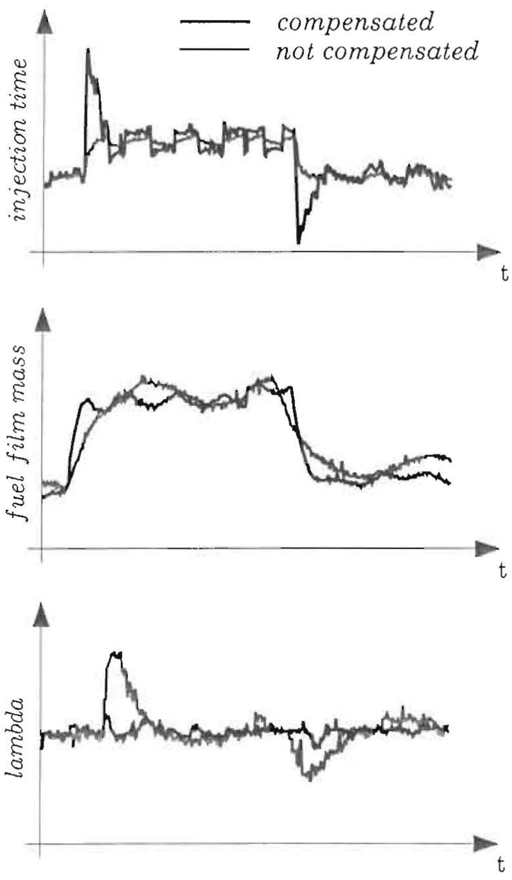

Figure 3.20 Compensation of fuel film dynamics at a test engine

angles increase the emission of NO_x. NO_x can be reduced by delaying the ignition at the expense of a higher fuel consumption [2]. The following parameters are used to control the ignition angle:

- Intake manifold pressure p_m
- Mass air flow $\dot{m}_a$
- Engine speed n
- Throttle angle α_t
- Air-fuel ratio λ

[2]Over all, the determination of the right ignition angle is a compromise between different objectives.

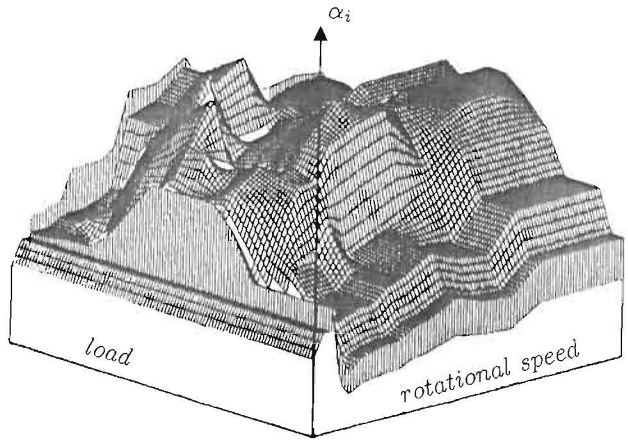

Figure 3.21 Ignition angle map

ignition angle is selected to minimise emissions, the fuel consumption will be higher. A compromise must consider fuel consumption and emission levels at all engine operating points. Emission levels can be very high at some particular operating points. There, the optimisation must focus on the emissions. Other operating points show acceptable emission rates. At these points the optimisation must focus on fuel consumption.

Fuel consumption and emission levels are measured in special road driving cycles like the ECE-test or FTP-test. These tests specify the vehicle velocity over time. Translating vehicle to engine speeds, a test cycle is equivalent to a sequence of different engine operating points over time. Every operating point is defined by several control parameters including engine speed and load.

The fuel consumption can be described by the volume $\dot{V}$ of combusted fuel over time. The minimisation criterium is the integral over the test cycle.

$$V = \int_0^T \dot{V}(t)\, dt \rightarrow min \tag{3.66}$$

The total fuel consumption V for a test cycle time T can also be obtained by a discrete summation over the engine operating points.

$$V = \sum_{i=1}^{N} \dot{V}_i(\alpha_i, \lambda_i)\, t_i \rightarrow min \tag{3.67}$$

An analysis of the test cycle shows that most operating points are visited several times. The individual time periods where the engine stays in the same operating point i can be summarised into a total time period t_i. The fuel consumption over time $\dot{V}_i$ can then be minimised independently for each operating point. The resulting values of α_i and λ_i are stored into look-up tables $\alpha_i(t_{inj}, n)$ and $\lambda_i(t_{inj}, n)$ for every operating point.

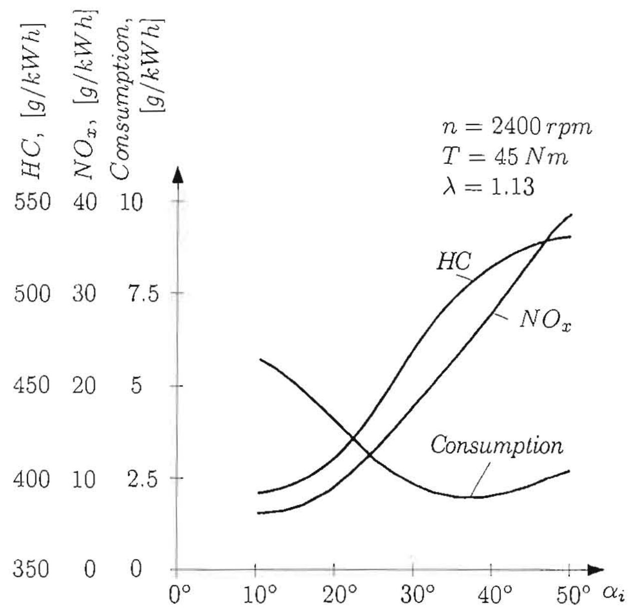

Figure 3.22 Fuel consumption and emission levels over ignition angle α_i.

When optimising fuel consumption, the maximum allowable emission levels are treated as optimisation constraints. The maximum emission rates are fixed by laws which specify the maximum integral masses of the different pollutants generated during a test cycle.

$$HC = \sum_{i=1}^{N} \dot{HC}(\alpha_i, \lambda_i)\, t_i \leq \hat{HC} \tag{3.68}$$

$$CO = \sum_{i=1}^{N} \dot{CO}(\alpha_i, \lambda_i)\, t_i \leq \hat{CO} \tag{3.69}$$

$$NO_x = \sum_{i=1}^{N} \dot{NO}_x(\alpha_i, \lambda_i)\, t_i \leq \hat{NO}_x \tag{3.70}$$

The emission levels per time $\dot{HC}, \dot{CO}, \dot{NO}$ can be influenced by the values of α_i and λ_i at each operating point i. The emission limits are only given for the integral mass over the whole test cycle. It is therefore not obvious which α_i and λ_i values must be adopted at each operating point i. Such an optimisation problem with constraints can be solved by using the Lagrange multiplication method [4]. The differences between actually achieved and acceptable emission levels are weighted by Lagrange factors L. Equation 3.67 and equations 3.68 to

3.70 are combined into a sinį

$W = V + L_{HC}(HC - \hat{HC})$

Now the cost function W mı
were at the acceptable limi
consumption would disappea
can be divided into two part
operating points i and a vari

$$W = \sum_{i=1}^{N} \dot{V}_i(\alpha_i, \lambda_i)t_i + \ldots$$
$$\sum_{i=1}^{N}[L_{HC}\dot{HC}(\alpha_i, \ldots$$
$$-L_{HC}\hat{HC} - L_C \ldots$$
$$W = \sum_{i=1}^{N} Z(\alpha_i, \lambda_i)t_i - \ldots$$

where:

$W_0 = L_{HC}\hat{H}\ldots$

and:

$Z(\alpha_i, \ldots$

The value of W can be minii
operating point:

Figure 3.23 shows $\dot{V}(\alpha_i, \lambda_i)$ a
on ignition angle α_i and air-fı
test bed run. The pair α_i, λ_i
It can be seen that fuel
slightly higher than the absolı
$\dot{NO}_x(\alpha_i, \lambda_i)$. The value W is
for the Lagrange factors L_{HC}
iterations with modified Lagr
which also meets the legal em
low fuel consumption V is att